Journal of Vacuum Science and Technology B

RESEARCH ARTICLE | OCTOBER 01 1983

Conventional novolak resists for storage ring x-ray lithography

J. G. Lane; J. R. Maldonado; A. N. Cleland; R. P. Haelbich; J. P. Silverman; J. M. Warlaumont

J. Vac. Sci. Technol. B 1, 1072–1075 (1983)
https://doi.org/10.1116/1.582679

06 July 2024 20:10:55

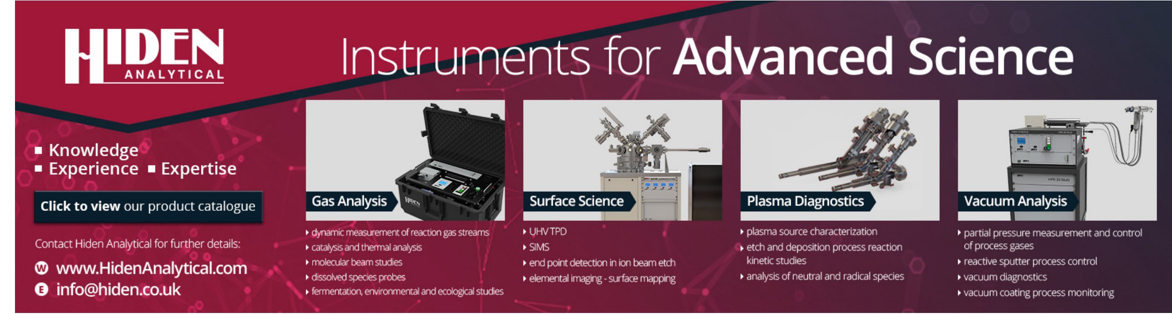

Conventional novolak resists for storage ring x-ray lithography

J. G. Lane,[a] J. R. Maldonado, A. N. Cleland,[b] R. P. Haelbich, J. P. Silverman, and J. M. Warlaumont

IBM Thomas J. Watson Research Center, Yorktown Heights, New York 10598

(Received 3 June 1983; accepted 13 September 1983)

This paper describes the lithographic processing of several positive novolak-based resists exposed on the IBM x-ray lithography system at the Brookhaven National Laboratory 750 MeV storage ring. One of the advantages of the storage ring exposure system has been the ability to use resist development processes which are the same as the corresponding optical or e-beam processes. The exposure system and the x-ray mask used for resist evaluation are described elsewhere in this symposium. Determining the best process conditions requires consideration of mask contrast as well as the desired linewidth and profile control, particularly in the presence of topography. Data will be presented and compared with results obtained using other lithographic systems (i.e., e-beam and conventional source x-ray). In particular, the relationship of mask absorber thickness to process window will be presented using a simple model of the development process. Using the process window defined by this model, we have exposed test patterns and typical device patterns in 1 to 2 μm thick conventional positive novolak resists. Linewidth control data as a function of dose and development time were determined for one resist at doses in the 100–200 mJ/cm^2 range and compared with corresponding results using electron beam exposure. The x-ray exposures compared favorably with the electron beam exposures in the dosage ranges considered.

PACS numbers: 07.85. + n, 85.40. − e

I. INTRODUCTION

One of the primary difficulties in taking advantage of the high resolution capability of x-rays has been the unavailability of high sensitivity resists which do not entail significant process complexities. As previously suggested,[1–3] use of storage ring generated x-rays not only improves resolution by reducing penumbra effects from small point sources but also provides a much brighter source. This makes x-ray lithograph feasible with a much wider range of resists including materials used for conventional optical and e-beam single level processing.[4]

A difficulty in beginning a lithography program using a novel exposure source is how best to select resist materials and how to determine the initial process window: of particular concern is the lack of completely opaque masking materials. To accomplish these tasks for a variety of novolak-based resists we have used exposures on a laboratory Al K_α source[2] and on the VUV synchrotron radiation storage ring at the National Synchrotron Light Source at Brookhaven National Laboratories. The Al K_α source provides a resist absorption spectrum similar to a dedicated x-ray lithography storage ring source and beam line[1] operating at about 1 GeV. A simple model of the development process was used to analyze development data from resists exposed on Si wafers. This model was then used to define a process window of minimum resist thinning (under the gold absorber area of an x-ray mask) as a function of incident dose, mask contrast, and development time.

II. DOSE CALIBRATION

X-ray doses have been determined from optical density changes in radiachromic dye-based dosimeter films which have been calibrated against a well characterized Al K_α source.[5] The optical density change was then used to calibrate a photoemission detector installed in the beam line.

Two masks have been used in the present work: one, a silicon-based mask with a 0.6 μm plated gold absorber pattern with approximately vertical walls was described previously[6]; two, a 2.5 μm thick Mylar film with blanket evaporated gold was used to obtain a range of exposure doses. Using the linear absorption coefficient for gold at 8.0 Å (4.2 μm^{-1}) gives a good fit to the dosimeter determined transmission for the 0, 0.2, 0.5, and 0.7 μm gold thicknesses. Defining mask contrast as the ratio of transmission in the clear to absorber regions yields a mask contrast of 12 for the patterned mask.

III. EXPERIMENT

Five novolak-based resists were used in these experiments: XR1, XR2, and XR3 are IBM experimental materials; AZ1400-022 and AZ4110 are commercially available (from Shipley and Azoplate,®). An outline of the resist processes is shown in Table I. In each case coating and development processes were chosen as closely as possible to pre-existing optical or e-beam processes: no process optimization was done specifically for the x-ray exposures. The resists were developed using a He–Ne laser as an optical thickness monitor with an optical band pass filter to eliminate low level exposure during development.

IV. DEVELOPMENT MODEL

A feature common to the thickness–time development curves is an initial plateau followed by transition to a constant development rate as shown in Fig. 1. We have approxi-

 © 1983 American Vacuum Society

06 July 2024 20:10:55

TABLE I. Resist process summary.

Process step	XR1	XR2	XR3	AZ1400-022	AZ4110
			Resist		
Wafer preclean			Acid preclean/DI water rinse		
Adhesion promoter			20% HMDS in freon/2 min vapor		
Apply			Spin apply/40 s		
Pre-exposure bake	105 °C 30 min	85 °C 30 min	80 °C 30 min	90 °C 30 min	90 °C 15 min
Exposure window (J/cm²)	0.1 to 0.6	0.8 to > 1.9	0.8 to > 2.2	1.2 to > 1.5	(> 2.4?)
Mask contrast	12	12	12	12	> 12
Postexposure bake	105 °C 20 min	None	None	None	None
Develop	1:4.5 AZ2401 21.5 °C	1:4.5 AZ2401 22 °C	1:4.5 AZ2401 22 °C	1:5.0 AZ351 24 °C	1:4.0 AZ400K 20 °C

mated the development curves for all five resists by a two piece linear fit characterized by the parameters induction time t_I and bulk development rate R_B. Induction time is calculated as the time at which a line with zero slope fit to the initial thickness points intersects a line fit to the final thickness points. Figures 2 and 3 show t_I and R_B versus dose for the five resists (note $t_I = 0$ for AZ4110). An exponential function was fit to the rate and induction time versus dose for each set of data in Figs. 2 and 3 and the result used to investigate the limits of usage of each resist under various conditions of mask contrast, incident dose, and development time.

In the following discussion, time will be expressed as a percentage development past end point, where end point is defined as the time to clear resist from a large exposed area of the wafer. Figure 4 shows remaining resist thickness in the unexposed region versus incident dose for resist XR1 at 50% past end point and for various mask contrasts. A significant feature of this curve is that exposing at too high a dose leads to thickness loss in the unexposed region. This results from the low dose received through the gold mask causing a reduction in induction time. Fixing development time at 50% past end point we see that a mask contrast of five or greater is required to allow a reasonably large process window for dose. Alternately, we can choose a development time of 50% past end point and a mask contrast of 12 (0.6 μm gold) and determine a dose window of 0.1 to 0.6 J/cm². The corresponding dose windows for the remaining resists (assuming mask contrasts as shown) are listed in Table I. AZ4110 has no acceptable process window at doses below the highest experimental dose of 2.4 J/cm².

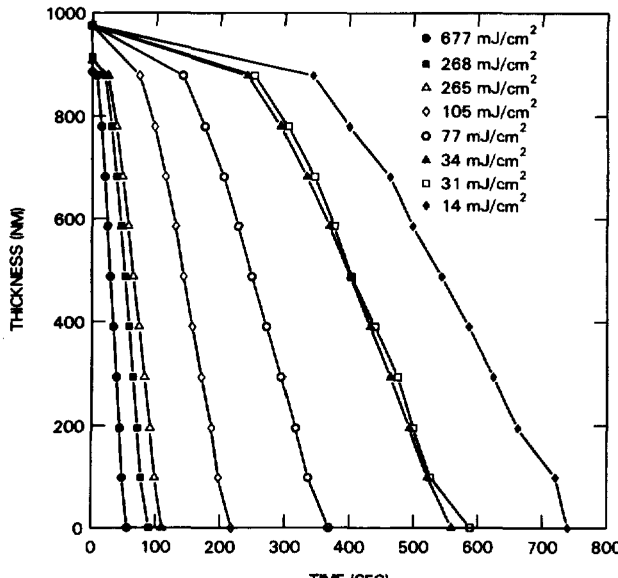

FIG. 1. Resist XR1 thickness vs development time for various storage ring x-ray doses in mJ/cm².

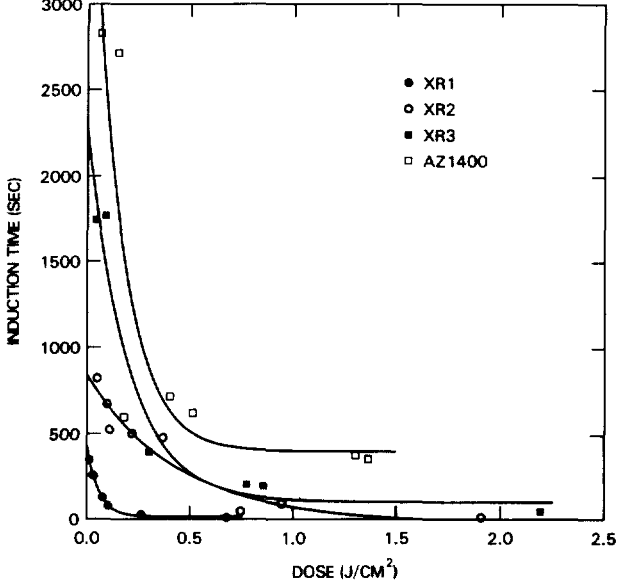

FIG. 2. Induction time vs dose for resists XR1, XR2, XR3, and AZ1400. AZ4110 has zero induction time.

06 July 2024 20:10:55

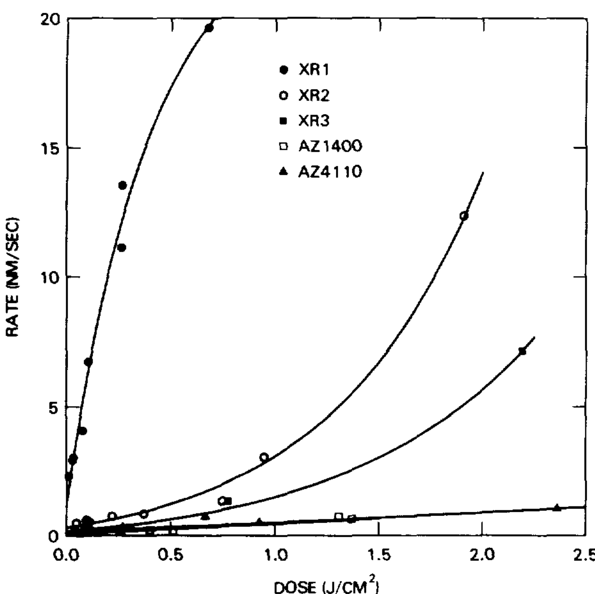

FIG. 3. Development rate vs dose for resists XR1, XR2, XR3, AZ1400, and AZ4110.

V. RESULTS

Using the process windows established from the model we have chosen doses for patterned exposures. Figure 5 shows a 0.75 μm line/space pattern in 1 μm of XR1 resist and a recessed oxide isolation device pattern in 2 μm thick XR1 resist.

Although initial dose uniformity over the mask field was on the order of $\pm$ 10%, the wide process window provides excellent linewidth control within a large portion of the exposure field. Figure 6 shows linewidths for resist XR1 over a range of 0.1 to 0.2 J/cm^2 and 0%–100% past end point with combined Al K_α and storage ring data. For comparison the linewidth over a smaller range is shown with e-beam exposure. The sensitivity of linewidth to dose and development time is better than for the corresponding e-beam exposure in a 5–10 μC/cm^2 range, particularly at shorter times past end point. Resist profile angles for storage ring exposures were generally greater than 85° and for the Al K_α source greater than 75° (due to penumbra).

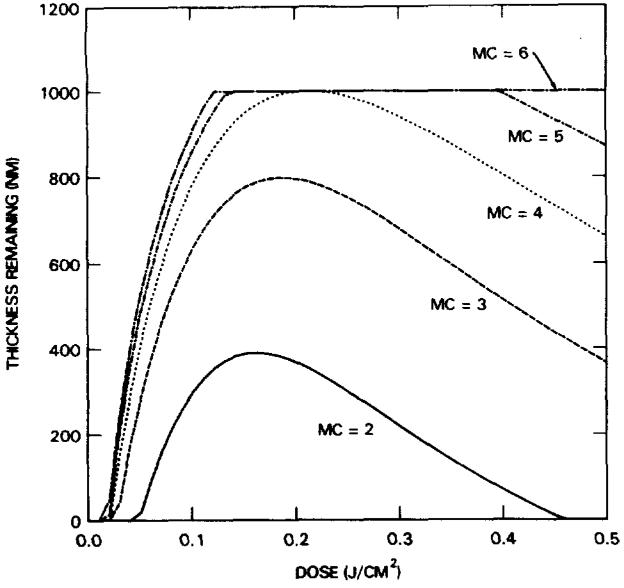

FIG. 4. Thickness remaining in the unexposed area vs dose for resist XR1 with development of 50% past end point for various mask contrasts (MC).

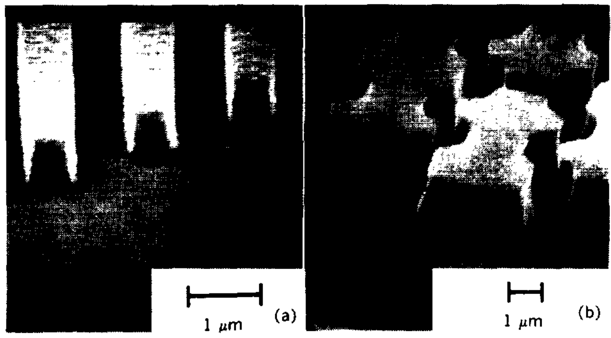

FIG. 5. Resist XR1 with storage ring exposure of 150 mJ/cm^2: (a) 0.75 μm line/space group in 1 μm thick resist, and (b) recessed oxide isolation pattern in 2 μm thick resist.

SEM measurements were made of 0.5–1.0 μm features over a 1×2 cm portion of the exposure field, with a pooled tolerance for 64 measurements of 3-sigma = 0.09 μm. This is within the estimated measurement repeatability of 3-sigma = 0.12 μm.

In addition to measurements of resist XR1 we have obtained images as shown in Fig. 7 for the other novolak-based resists with resolution down to 0.4 μm in 1 μm thickness. Figure 8 shows excellent imaging of XR1 over steps of about 0.3 μm.

VI. CONCLUSION

A simple model of the development process of x-ray exposed resists was used to define the initial process window for a number of conventional novolak-based resists. The process window was used to define storge ring exposure doses for patterned resist exposures and the resulting process sen-

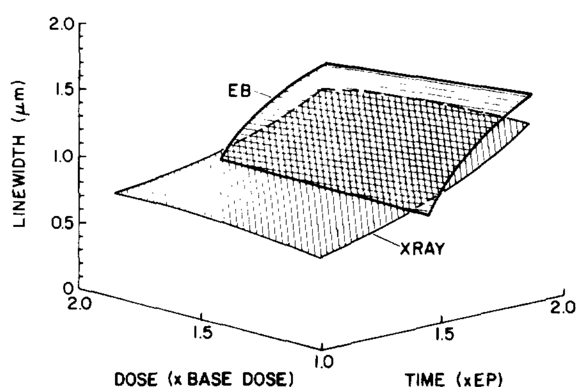

FIG. 6. Linewidth dependence on dose and development time for combined storage ring and Al K_α x-ray data at 100 mJ/cm^2 base dose and for e-beam data at 5 μC/cm^2 base dose for resist XR1. EP is time for development end point.

06 July 2024 20:10:55

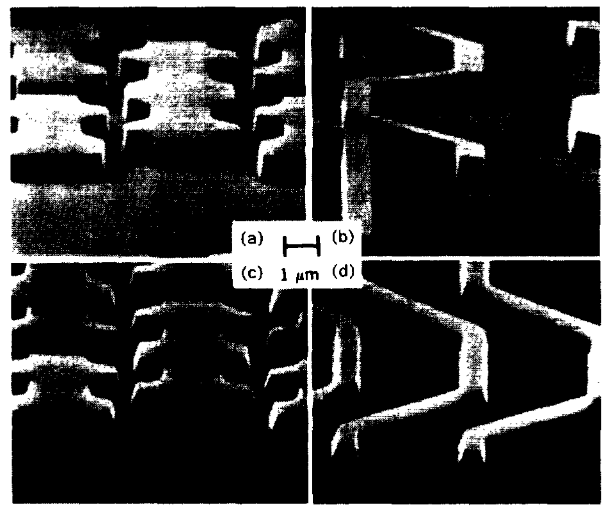

FIG. 7. Recessed oxide isolation (left) and FET metallization (right) patterns in 1 μm thick resists exposed on the storage ring: (a) XR2 at 2.0 J/cm², (b) XR3 at 1.6 J/cm², (c) AZ4110 at 1.0 J/cm², and (d) AZ1400-022 at 1.6 J/cm².

sitivity and linewidth control were measured for one of the resists.

Results define requirements for mask contrast and demonstrate excellent linewidth control as well as decreased sensitivity to process parameters compared to e-beam exposure. Finally, we have made initial exposures over topography and shown that the wide process window allows good lithographic performance over such features.

ACKNOWLEDGMENTS

We would like to thank Warren Grobman for his past support and encouragement of the beam line project, Dino Costas for his technical assistance at the beam line, and Rob Metz and Rob Gazdzinski for their assistance with the resist process work. In addition we would like to acknowledge the help of the individuals in the East Fishkill IBM Development Laboratory who provided the development processes for the resists used in this study, and of Alan Wilson and the members of the Yorktown Chip Lithography group who provided the x-ray mask and support for the beam line exposure system. Finally, we would like to acknowledge DARPA for partial support for this work under contract N00014-82-C-2094 and the staff of the National Synchrotron Light Source for their cooperation in providing the x-ray source.

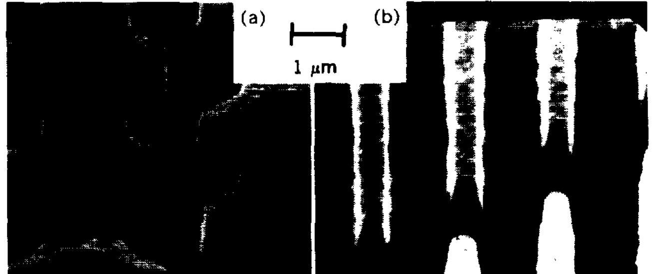

FIG. 8. Resist XR1 over approximately 0.3 μm steps at 100 mJ/cm² (Al K_α source): (a) oxide/nitride to oxidized Si step, and (b) reoxidized polysilicon to polysilicon step.

[a] Permanent address: IBM East Fishkill, Hopewell Junction, NY 12533.
[b] Presently at the University of California at Berkeley.

[1] J. P. Silverman, R. P. Haelbich, W. D. Grobman, and J. M. Warlaumont, Proceedings of SPIE: Electron-Beam, X-ray & Ion-Beam Techniques for Submicron Lithographies II **393**, 99 (1983).

[2] J. M. Warlaumont and J. R. Maldonado, J. Vac. Sci. Technol. **19**, 1200 (1981).

[3] H. Aritome, S. Matsui, K. Moriwaki, and S. Namba, J. Vac. Sci. Technol. **16**, 1939 (1979).

[4] T. Kimura, K. Mochiji, N. Tsumita, H. Obayashi, A. Mikuni, and H. Kanzaki, in Proc. SPIE: Electron-Beam, X-Ray & Ion-Beam Techniques for Submicron Lithographies II **393**, 2 (1983).

[5] J. M. Shaw and M. Hatzakis, J. Vac. Sci. Technol. **19**, 1343 (1981).

[6] R. E. Acosta, J. M. Warlaumont, and R. G. Viswanathan, presented at 1983 International Symposium on Electron, Ion and Photon Beams, Los Angeles, 1983.

06 July 2024 20:10:55